**ESI for**

# Compositionally Tunable Ternary $Bi_2(Se_{1-x}Te_x)_3$ and $(Bi_{1-y}Sb_y)_2Te_3$ Thin Films via Low Pressure Chemical Vapour Deposition

Sophie L. Benjamin[a,b], C. H. (Kees) de Groot[c], Chitra Gurnani[a,d], Samantha L. Hawken[a], Andrew L. Hector[a], Ruomeng Huang[c*], Marek Jura[e], William Levason[a], Eleanor Reid[a], Gillian Reid[a*], Stephen P. Richards[a], Gavin B. G. Stenning[e]

***Experimental Section:***

***Precursor synthesis***

All precursor complexes were prepared using Schlenk, vacuum line and glove box techniques under a dry nitrogen atmosphere. The reagents were stored and manipulated using a dry, $N_2$-purged glove box. MeCN and $CH_2Cl_2$ were dried by distillation from $CaH_2$. $Se^nBu_2$,[1] $Te^nBu_2$[2] and $[BiCl_3(Te^nBu_2)_3]$[3] were prepared according to the literature methods. IR spectra were recorded as Nujol mulls between CsI plates using a Perkin-Elmer Spectrum 100 instrument unless otherwise stated and $^1H$ and $^{13}C\{^1H\}$ NMR spectra were recorded from solutions in $CDCl_3$ or $CD_2Cl_2$ on a Bruker AV400 spectrometer, $^{77}Se\{^1H\}$ and $^{125}Te\{^1H\}$ NMR spectra on a Bruker AV400 spectrometer referenced to external neat $SeMe_2$ and $TeMe_2$, respectively. Microanalytical results were obtained from Medac Ltd. Note that the yields quoted are those corresponding to the final isolated materials and reflect losses in removing the oils from the Schlenk flasks.

**$[BiCl_3(Se^nBu_2)_3]$:** $BiCl_3$ (0.10 g, 0.32 mmol) was dissolved in anhydrous MeCN (10 mL) and the solution cooled to 0 °C. A solution of $Se^nBu_2$ (0.18 g, 0.96 mmol) in MeCN (10 mL) was slowly added, giving a pale yellow solution which was allowed to warm to room temperature and then stirred for 1 h. The volatile components were removed *in vacuo*, leaving a viscous yellow oil that was dried *in vacuo* for 1 h. Yield: 0.19 g, 68 %. $^1H$ NMR ($CDCl_3$): δ = 0.95 (*t*, [3H], $CH_3$), 1.46 (*m*, [2H], $CH_2$), 1.72 (*q*, [2H], $CH_2$), 2.99 (*t*, [2H], $CH_2Se$). $^{13}C\{^1H\}$ NMR ($CDCl_3$): δ = 13.6 ($CH_3$), 23.0 ($CH_2$), 27.2 ($CH_2$), 32.6 ($CH_2Se$). $^{77}Se\{^1H\}$ NMR ($CH_2Cl_2/CDCl_3$): δ = 196. IR (neat thin film /$cm^{-1}$): *v* = 267 br (Bi–Cl). Anal. calcd for $C_{24}H_{54}BiCl_3Se_3$: C 32.2, H 6.1; found: C 31.9, H 6.2%.

[a] Chemistry, University of Southampton, Southampton SO17 1BJ, U.K. Email: G.Reid@soton.ac.uk
[b] School of Science and Technology, Nottingham Trent University, Nottingham NG11 8NS, U.K.
[c] Electronics and Computer Science, University of Southampton, Southampton SO17 1BJ, U.K. Email: R.Huang@soton.ac.uk
[d] School of Natural Sciences, Mahindra Ecole Centrale, Hyderabad, India.
[e] ISIS Neutron and Muon Source, Rutherford Appleton Laboratory, Harwell Science and Innovation Campus, Didcot, OX11 0QX, UK.

**[$SbCl_3(Se^nBu_2)_3$]:** Freshly sublimed $SbCl_3$ (0.228 g, 1.0 mmol) was dissolved in anhydrous MeCN (10 mL) and the solution cooled to 0 °C. A solution of $Se^nBu_2$ (0.580 g, 3.0 mmol) in MeCN (10 mL) was slowly added, giving a pale yellow solution which was allowed to warm to room temperature and then stirred for 1 h. The volatile components were removed *in vacuo*, leaving a pale yellow oil that was dried gently *in vacuo*. $^1$H NMR ($CDCl_3$): δ = 0.91 (*t*, [3H], $CH_3$), 1.39 (*m*, [2H], $CH_2$), 1.63 (*q*, [2H], $CH_2$), 2.54 (*t*, [2H], $CH_2Se$). $^{13}C\{^1H\}$ NMR ($CDCl_3$): δ = 13.9 ($CH_3$), 23.6 ($CH_2$), 24.4 ($CH_2$), 33.3 ($CH_2Se$). $^{77}Se\{^1H\}$ NMR ($CH_2Cl_2$): δ = 168. IR (thin film/$cm^{-1}$): *ν* = 306 br (Sb−Cl). Anal. calcd for $C_{24}H_{54}SbCl_3Se_3$: C 35.69, H 6.74; found: C 34.54, H 7.25%.

**[$SbCl_3(Te^nBu_2)_3$]:** $SbCl_3$ (0.228 g, 1.0 mmol) was directly reacted with $Te^nBu_2$ (0.725 g, 3.0 mmol) at room temperature, giving a dark orange/red oil; volatiles were removed . Yield: 0.19 g, 68%. $^1$H NMR ($CDCl_3$): δ = 0.92 (*t*, [3H], $CH_3$), 1.41 (*m*, [2H], $CH_2$), 1.71 (*q*, [2H], $CH_2$), 2.72 (*t*, [2H], $CH_2Te$). $^{13}C\{^1H\}$ NMR ($CDCl_3$): δ = 4.28 ($CH_2Te$), 13.5 ($CH_3$), 25.8 ($CH_2$), 34.9 ($CH_2$). $^{125}Te\{^1H\}$ NMR ($CH_2Cl_2$): δ = 237. IR (neat thin film /$cm^{-1}$): *ν* = 248 br (Sb−Cl). Anal. calcd for $C_{24}H_{54}SbCl_3Te_3$: C 30.2, H 5.7; found: C 29.9, H 5.7%.

***Low Pressure CVD experiments***

Physical vapour deposited (PVD) $SiO_2$ on Si substrates were prepared as described previously.[4] In a typical experiment, the reagent, followed by the PVD silica substrate tiles (usually at least four tiles of 0.5 x 8 x 20 mm) were placed edge-to-edge lengthways in a closed-end silica tube in a glovebox. The amount of precursor used was typically 40-60 mg. The tube was placed horizontally in a Lenton tube furnace (total length = 36 cm of which the central 30 cm is heated) such that the precursor protruded *ca.* 2 cm beyond the furnace edge. The tube was evacuated to 0.05 – 0.1 mm Hg. The furnace was then heated to the desired temperature (producing a temperature gradient that was profiled between experiments) and the temperature across the tube was allowed to stabilise. The tube was then repositioned to move the precursor closer to the heated zone until evaporation could be observed. The temperatures at which the precursors vaporised sufficiently rapidly for effective thin film growth were measured as: $Bi_2Te_3$: 240 °C; $Sb_2Te_3$: 270 °C; $Sb_2Se_3$: 280-300 °C; $Bi_2Se_3$: 280-300 °C; combined $Bi_2Te_3$ / $Bi_2Se_3$: 290-300 °C; combined $Bi_2Te_3$/ $Sb_2Te_3$: 270 °C. The position of the tube was maintained until the precursor was completely consumed), usually *ca.* 1 h. Once complete, the tube was allowed to cool to room temperature and transferred to the glove box. The substrates were removed and stored under $N_2$ before characterisation. For depositions of $Bi_2(Se_{1-x}Te_x)_3$ ternary thin films, appropriate ratios of $[BiCl_3(E^nBu_2)_3]$ (E =Se, Te) were first mixed in $CH_2Cl_2$ and then transferred to the silica CVD tube. The tube was set in the furnace such that the precursor protruded 2 cm beyond the edge of the furnace. The tube was carefully evacuated (0.05 mm Hg), whereby the $CH_2Cl_2$ was gradually evaporated, and then the system was ramped up to 550 °C. The tube position was then adjusted so that the precursor was moved towards the heated zone until evaporation was observed. After 1 h, the tube was cooled to room temperature and transferred to the glovebox, where the tiles were removed and stored under an $N_2$ atmosphere prior to analysis. The thin film deposits on the substrates were dark grey in appearance. The

highest degree of substrate coverage occurred on the tiles closest to the precursor. The films were generally very well adhered to the tiles (except for the $Sb_2Se_3$ which were very fragile).

***Thin Film Characterisation***

X-ray diffraction (XRD) measurements were carried out using a Rigaku SmartLab diffractometer with a 9 kW Cu-$K_\alpha$ source, parallel line incident beam and a DTex250 1D detector. The crystalline phase of the films was determined by matching to a literature XRD pattern and lattice parameters calculated by further optimisation of the fit using PDXL.[5] Raman scattering spectra of the deposited films were measured at room temperature on a Renishaw InVia Micro Raman Spectrometer using a helium-neon laser with a wavelength of 633 nm. The incident laser power was adjusted to ~1 mW for all samples. Scanning electron microscopy (SEM) and energy dispersive X-ray (EDX) measurements used a Zeiss EVO LS 25 with an Oxford INCAx-act X-ray detector, or a JEOL JSM 6500 F Field Emission Scanning Electron Microscope with an INCA x-sight 7418 EDX probe with an accelerating voltage of 10 kV. High resolution SEM measurements used a field emission SEM (Jeol JSM 7500F) at an accelerating voltage of 2 kV.

Van der Pauw and Hall measurements were performed at room temperature on a Nanometrics HL5500PC at 300 K. The latter used a field of 0.5 Tesla. For each measurement, four copper probes with diameter of *ca*. 1 mm were carefully placed on the sample corners. Care was taken to ensure linear contact was obtained between each probe and the sample before each measurement.

***Results and Discussion:***

***Binary precursors and their characterisation:*** The six-coordinate Sb(III) complexes, $[SbCl_3(E^nBu_2)_3]$ (E = Se, Te), were isolated in good yields as yellow (Se) and red (Te) oils, respectively, whilst the $[BiCl_3(Se^nBu_2)_3]$ was an orange oil. Samples were handled in an $N_2$ purged glove box and could be stored in a freezer (−18 °C) for several weeks. Characterisation of new precursors by IR spectroscopy, $^1$H, $^{13}$C{$^1$H}, $^{77}$Se{$^1$H} and $^{125}$Te{$^1$H} nuclear magnetic resonance (NMR) spectroscopy and microanalysis are consistent with a distorted octahedral coordination environment. IR spectroscopy shows strong and broad peaks corresponding to the Bi-Cl and Sb-Cl stretches; at 271 $cm^{-1}$ for $[BiCl_3(Se^nBu_2)_3]$, and at 306 and 294 $cm^{-1}$ for $[SbCl_3(Se^nBu_2)_3]$ and $[SbCl_3(Te^nBu_2)_3]$, respectively, consistent with literature data for similar complexes.[6,7] The $^1$H NMR spectra of $[SbCl_3(Se^nBu_2)_3]$ and $[SbCl_3(Te^nBu_2)_3]$ ($CD_2Cl_2$) are very little shifted from the 'free' ligand, consistent with the complexes being highly labile and extensively dissociated in solution. The $[BiCl_3(Se^nBu_2)_3]$ exhibits a larger high frequency shift, most notably for the $CH_2$ groups adjacent to the Se donor atom (complex: $\delta$ = 3.11; ligand: $\delta$ = 2.57 ppm), consistent with $BiCl_3$ being a stronger Lewis acid than $SbCl_3$. The $^{13}$C{$^1$H}, $^{77}$Se{$^1$H} and $^{125}$Te{$^1$H} NMR spectra show similar trends (Table S1).

Table S1: $^{77}Se\{^{1}H\}$ and $^{125}Te\{^{1}H\}$ NMR spectroscopic data ($CH_2Cl_2$, 298 K).

| Compound | $\delta(^{77}Se)$ / ppm | $\delta(^{125}Te)$ / ppm |
|---|---|---|
| $Se^nBu_2$ | 167 | – |
| $[BiCl_3(Se^nBu_2)_3]$ | 196 | – |
| $[SbCl_3(Se^nBu_2)_3]$ | 168 | – |
| $Te^nBu_2$ | – | 238 |
| $[BiCl_3(Te^nBu_2)_3]$ | – | 262 |
| $[SbCl_3(Te^nBu_2)_3]$ | – | 237 |

***LPCVD of binary $M_2E_3$ (M = Sb, Bi; E = Se, Te) thin films:*** LPCVD experiments using each of the new precursors individually, established their suitability for the growth of silvery grey crystalline $M_2E_3$ films, and these were characterised by grazing incidence XRD, Raman spectroscopy, SEM and EDX analysis. Refined lattice parameters (Table S2) are in good agreement with literature data. For $Bi_2Se_3$, LPCVD experiments were typically performed at 550 °C/0.05 mmHg, since at 500 °C a mixture of phases (predominantly BiSe and $Bi_3Se_4$) was produced, without any evidence for $Bi_2Se_3$, whereas, increasing the temperature to 600 °C resulted in evaporation of the precursor, without any significant deposition onto the substrates. The phase pure $Bi_2Se_3$ films deposited at 550 °C were *ca*. 1 μm thick (Figs. S1 and S2).

Energy dispersive X-ray (EDX) analysis shows a Bi: Se ratio of 41.7 % : 58.3 %. Raman spectroscopy (Fig. S2b) shows two peaks at 130 and 172 $cm^{-1}$. These can be assigned as the $E_g^2$ (in plane) and the $A_{1g}^2$ (out of plane) vibrational modes, respectively, consistent with literature values.[8]

$Sb_2Se_3$ films were deposited using *ca.* 30 mg of $[SbCl_3(Se^nBu_2)_3]$ at 525, 550 and 575 °C (0.1 mm Hg), leading to complete evaporation of the precursor. The films produced were quite poorly adhered to the substrate (Fig. S3), with SEM images revealing a random orientation of rod- or needle-like crystallites. Quantitative EDX analysis showed that the films were within experimental error of the expected 2:3 Sb:Se stoichiometry (41% Sb : 59% Se), with no evidence for residual Cl. The lower temperature (525 °C) appears best suited for the deposition of $Sb_2Se_3$ from this precursor. The Raman spectrum (Fig. S4b) shows peaks at 125, 150 and 190 $cm^{-1}$, representing the $E_g^2$, $A^2{}_{2u}$ and $A_{1g}^2$ modes, respectively, from $Sb_2Se_3$. The $E_g^2$ mode relates to the Se-Se bonds, the $A^2{}_{2u}$ to the vibration of Sb-Sb bonds, while the $A_{1g}^2$ mode represents Sb–Se stretching mode of the $SbSe_{3/2}$-pyramids.[9-12]

For $Sb_2Te_3$ films, initial depositions used $[SbCl_3(Te^nBu_2)_3]$ at 450 °C and 500 °C onto $SiO_2$ substrates. The precursor was positioned about 2 cm beyond the edge of the furnace and gradually moved closer until sublimation was observed. However, this resulted in the co-deposition of $Sb_2Te_3$ and crystalline tellurium. Adaptation of the method, where the CVD tube was repositioned such that once the required furnace

temperature was reached, the precursor was moved rapidly to the edge of the hot zone, allowed for 'flash evaporation' of the precursor. This allowed $Sb_2Te_3$ films to be obtained without co-deposition of elemental tellurium. At 450 °C the small crystallites deposited are very scattered and the film is not continuous (Figure S5a). Increasing the temperature to 500 °C to increase nucleation led to continuous films of $Sb_2Te_3$ being produced. SEM analysis of the films produced at 450 °C shows the crystallites to be *ca.* 100 nm in diameter, whilst those grown at 500 °C are *ca.* 1 µm across, and the substrate coverage is much higher (Fig. S5b). In comparison with $Sb_2Te_3$ films deposited from $MeSb(Te^nBu_2)_2$,[9] the films deposited from the new $[SbCl_3(Te^nBu_2)_3]$ precursor do not show any significant preferred orientation, with some crystallites lying flat and some perpendicular to the substrate. The elemental composition of the $Sb_2Te_3$ film was also probed by EDX analysis, showing an Sb:Te ratio of 38 % : 62 %, within experimental error of that expected for $Sb_2Te_3$. There is no evidence for Cl incorporation into the film. The Raman spectrum (Fig. S6b) of the film shows peaks at 120, 140 and 165 $cm^{-1}$, attributed to the $E_{2g}$, $A_{2u}$ and $A_{1g}$ vibrational modes expected from $Sb_2Te_3$.[13]

The electrical properties of the binary $M_2E_3$ films were investigated by Hall (or, for $Sb_2Se_3$, van der Pauw) measurements (Table S2), showing that $Sb_2Te_3$ is a p-type semiconductor, whilst $Sb_2Se_3$, $Bi_2Se_3$ and $Bi_2Te_3$ are n-type. $Sb_2Te_3$ has a very low resistivity (1.26 x $10^{-3}$ Ω cm), in good agreement with literature data.[9,14,15] Similarly, Hall measurements show that $Bi_2Se_3$ also has a low resistivity (8.3 x $10^{-4}$ Ω cm), with a mobility of 4.2 $cm^2/C$ and carrier density of 2.18 x $10^{21}$ $cm^{-3}$.

Table S2. Lattice parameters and electrical data for $M_2E_3$ films with $Bi_2Se_3$, $Bi_2Te_3$ and $Sb_2Te_3$ adopting the $Bi_2Se_3$ structure type (*R*-3*mH*) and $Sb_2Se_3$ the $Sb_2S_3$ type (*Pnma*).

| Precursor | Thin Film Deposit | a / Å | b / Å | c / Å | Type | Resistivity / Ωcm | Mobility µ / $cm^2V^{-1}S^{-1}$ | Carrier Concentration N / $cm^{-3}$ | Ref. |
|---|---|---|---|---|---|---|---|---|---|
| $[BiCl_3(Se^nBu_2)_3]$ | $Bi_2Se_3$ | 4.092(14) | 4.092(14) | 28.59(11) | N | 8.3 x $10^{-4}$ | 4.2 | 2.18 x $10^{21}$ | This work |
| $[BiCl_3(Te^nBu_2)_3]$ | $Bi_2Te_3$ | 4.378(10)<br>4.3823(19) | 4.378(10)<br>4.3823(19) | 30.46(5)<br>30.498(17) | N<br>- | 5.65(2) x $10^{-4}$<br>- | 56.6<br>- | 1.95 x $10^{20}$<br>- | 3<br>This work |
| $[SbCl_3(Se^nBu_2)_3]$ | $Sb_2Se_3$ | 11.76(7) | 3.938(15) | 11.76(6) | -* | 8.4(2) x $10^4$ | -* | -* | This work |
| $[SbCl_3(Te^nBu_2)_3]$ | $Sb_2Te_3$ | 4.254(3) | 4.254(3) | 30.31(5) | P | 1.26(1) x $10^{-3}$ | 78.7 ± 1.3 | 6.3(1) x $10^{19}$ | This work |

* the low density of the orthorhombic $Sb_2Se_3$ films deposited was such that reliable Hall measurements were not possible, hence van der Pauw measurements of resistivity were undertaken.

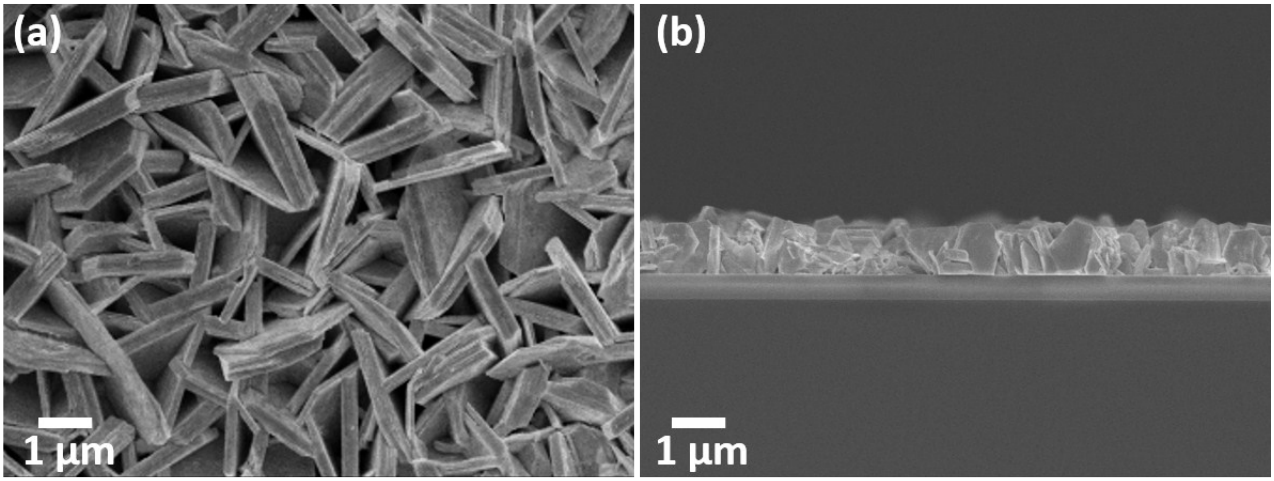


Figure S1: (a) Top view and (b) cross sectional SEM images of $Bi_2Se_3$ film deposited from $[BiCl_3(Se^nBu_2)_3]$ at 550 °C onto $SiO_2$.

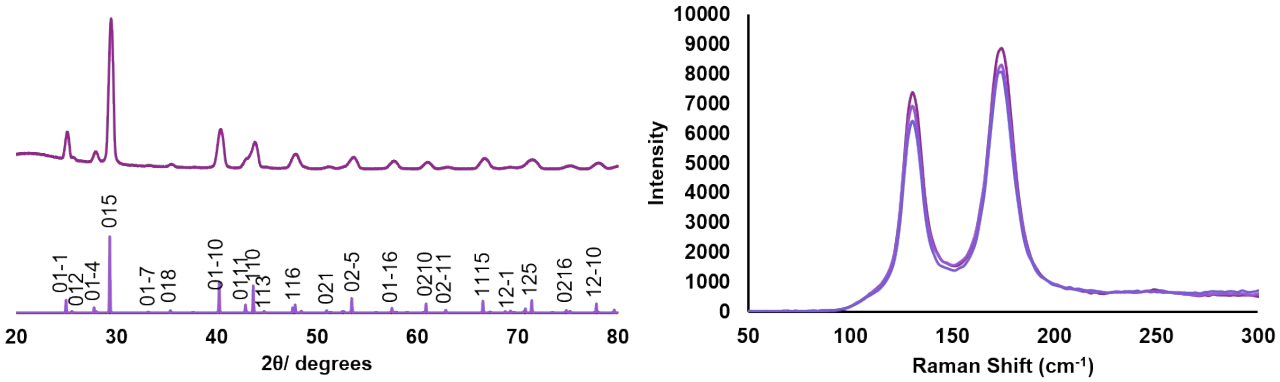


(a) (b)

Figure S2: (a) Grazing incidence XRD pattern for $Bi_2Se_3$ film deposited from $[BiCl_3(Se^nBu_2)_3]$ at 550 °C onto fused $SiO_2$ and an indexed pattern from bulk $Bi_2Se_3$; (b) Raman spectra recorded at different regions of the film.

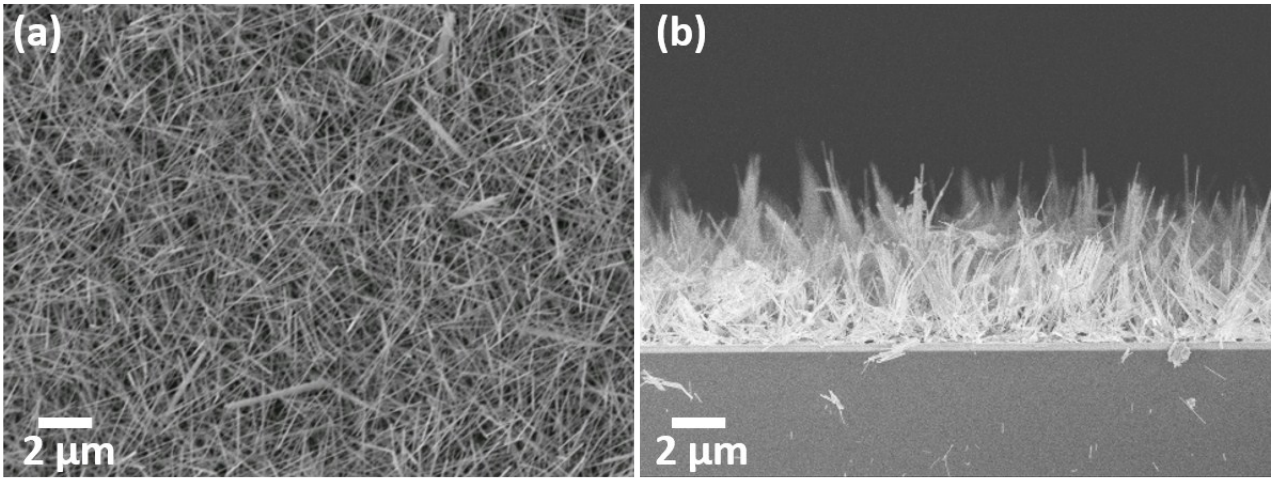


Figure S3: (a) Top views and (b) cross sectional SEM images of $Sb_2Se_3$ film deposited from $[SbCl_3(Se^nBu_2)_3]$ at 550 °C onto $SiO_2$.

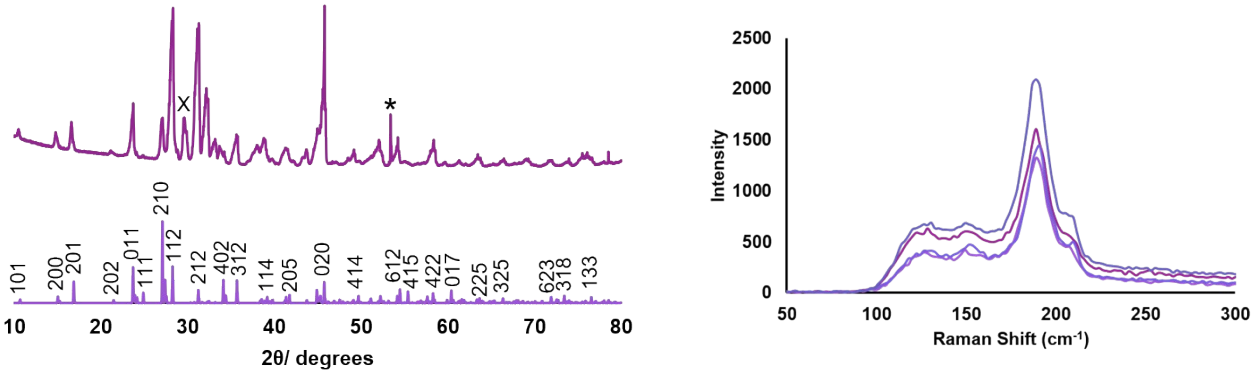


(a) (b)

Figure S4: (a) Grazing incidence XRD pattern for $Sb_2Se_3$ film deposited from $[SbCl_3(Se^nBu_2)_3]$ at 550 °C onto $SiO_2$ with an indexed pattern for bulk $Sb_2Se_3$.[8] The reflection marked with * is due to the underlying Si in the substrate and the peak marked X is due to an unknown impurity; (b) Raman spectra from several regions of the same film.

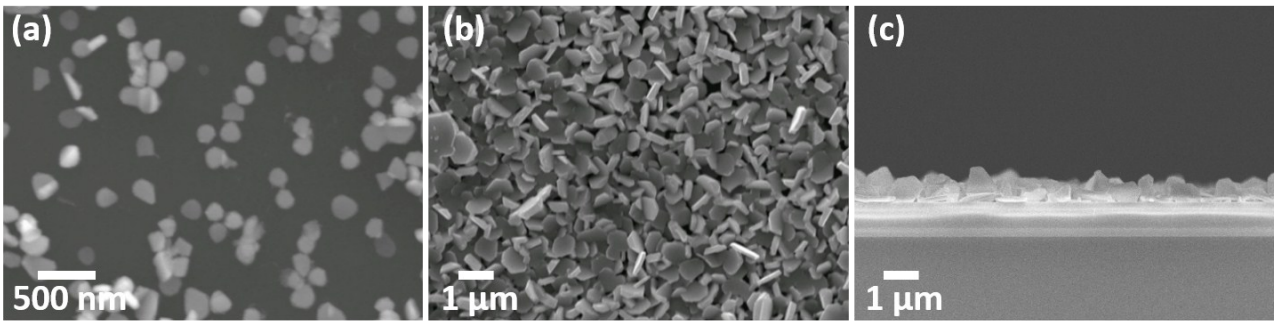


Figure S5: (a) SEM image of $Sb_2Te_3$ deposited from $[SbCl_3(Te^nBu_2)_3]$ at 450 °C; (b) 500 °C onto PVD $SiO_2$; (c) cross sectional SEM (from film deposited at 500 °C)

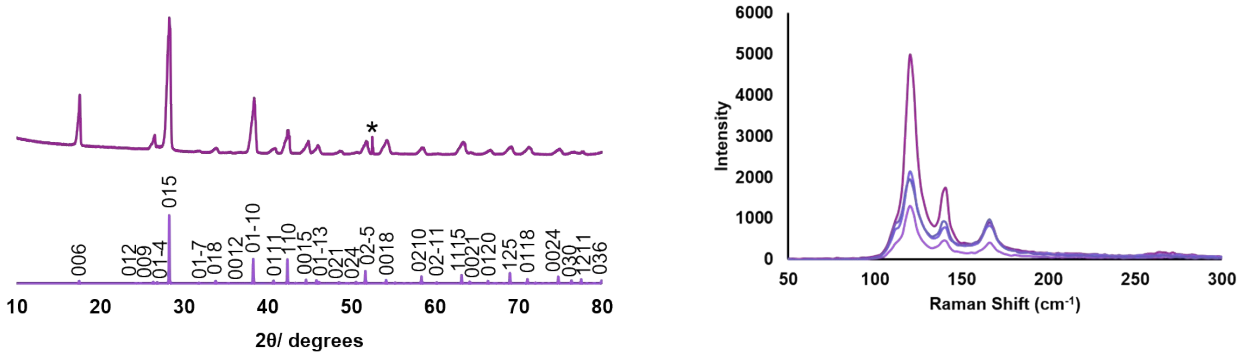


(a) (b)

Figure S6: (a) Grazing incidence XRD pattern from the $Sb_2Te_3$ film deposited from $[SbCl_3(Te^nBu_2)_3]$ at 500 °C onto $SiO_2$, together with an indexed pattern from bulk $Sb_2Te_3$.[13] The reflection marked * is from the underlying silicon substrate; (b) Raman spectra obtained from different regions of the same film.

**Ternary precursor systems: NMR experiments**

Samples of $[BiCl_3(Se^nBu_2)_3]$ and $[BiCl_3(Te^nBu_2)_3]$ were prepared freshly and a stock solution of each was prepared in anhydrous $CH_2Cl_2$ (0.033 mmol/mL), henceforth termed 'Se stock' and 'Te stock' respectively. In each of four 10 mm NMR tubes were mixed 1.5 mL of $CDCl_3$ with one of: (i) 1.5 mL of Te stock; (ii) 1.0 mL of Te stock with 0.5 mL of Se stock; (iii) 0.5 mL of Te stock and 1.0 mL of Se stock; (iv) 1.5 mL of Se stock. The colour of the solutions graduated from red (entirely Te) through orange (mixtures of Se and Te) to yellow (entirely Se) (Figure S7). $^{77}Se\{^1H\}$ and $^{125}Te\{^1H\}$ NMR spectra (as appropriate) were collected at room temperature (Figure S7).

A similar approach was adopted for the ternary $(Bi_{1-y}Sb_y)_2Te_3$ using samples of $[SbCl_3(Te^nBu_2)_3]$ and $[BiCl_3(Te^nBu_2)_3]$ (Figure S8)

| **NMR sample:**<br>**Te:Se molar ratio:** | **(i)**<br>**1:0** | **(ii)**<br>**2:1** | **(iii)**<br>**1:2** | **(iv)**<br>**0:1** |
|---|---|---|---|---|
| $\delta(^{77}Se)$ / ppm | - | 162 | 169 | 196 |
| $\delta(^{125}Te)$ /ppm | 262 | 264 | 300 | - |

Figure S7: Showing the variation in the colours of precursor solutions (**i**) to (**iv**) (left to right) as a function of the ratio of $[BiCl_3(Te^nBu_2)_3]$ to $[BiCl_3(Se^nBu_2)_3]$ and their corresponding $^{77}Se\{^1H\}$ and $^{125}Te\{^1H\}$ NMR data ($CH_2Cl_2$, 298 K).

| **NMR sample:** | **(i)** | **(ii)** | **(iii)** | **(iv)** | **(v)** |
|---|---|---|---|---|---|
| **Bi:Sb molar ratio:** | **1:0** | **2:1** | **1:1** | **1:2** | **0:1** |
| $\delta(^{125}Te)$ /ppm | 262 | 250 | 246 | 238 | 237 |

Figure S8: Showing the variation in the colours of precursor solutions (**i**) to (**v**) (left to right) as a function of the ratio of of $[BiCl_3(Te^nBu_2)_3]$ and $[SbCl_3(Te^nBu_2)_3]$ in $CH_2Cl_2$ and their corresponding $^{125}Te\{^1H\}$ NMR chemical shift data.

Table S1 Refined lattice parameters of $Bi_2(Se_{1-x}Te_x)_3$ and $(Bi_{1-y}Sb_y)_2Te_3$ ternary films.

| **$Bi_2(Se_{1-x}Te_x)_3$ films** | **a / Å** | **c / Å** | **$(Bi_{1-y}Sb_y)_2Te_3$ films** | **a / Å** | **c / Å** |
|---|---|---|---|---|---|
| x = 0 | 4.140(3) | 28.58(4) | Position A | 4.370(11) | 30.80(8) |
| x= 0.2 | 4.174(16) | 28.89(9) | Position B | 4.327(8) | 30.54(8) |
| x= 0.5 | 4.248(5) | 29.76(5) | Position C | 4.249(9) | 30.29(8) |
| x= 0.7 | 4.295(9) | 29.89(5) | | | |
| x= 1.0 | 4.382(2) | 30.50(2) | | | |

## References


1. D. J. Gulliver, E. G. Hope, W. Levason, S. G. Murray, D. M. Potter and G. L. Marshall, *J. Chem. Soc., Perkin Trans.,* 1984, **2**, 429–434.
2. E. G. Hope, T. Kemmitt and W. Levason, *Organometallics*, 1988, **7**, 78–83.
3. S. L. Benjamin, C. H. de Groot, C. Gurnani, A. L. Hector, R. Huang, E. Koukharenko, W. Levason and G. Reid, *J. Mater. Chem. A*, 2014, **2**, 4865–4869.
4. C. H. de Groot, C. Gurnani, A. L. Hector, R. Huang, M. Jura, W. Levason and G. Reid, *Chem. Mater.*, 2012, **24**, 4442–4449.
5. S. Grazulis, D. Chateigner, R. T. Downs, A. F. Yokochi, M. Quiros, L. Lutterotti, E. Manakova, J. Butkus, P. Moeck and A. Le Bail, A., *J. Appl. Crystallogr*., 2009, **42**, 726–729.
6. (a) A. J. Barton, A. R. J. Genge, W. Levason and G. Reid, *J. Chem. Soc., Dalton Trans*., 2000, 859–865; (b) W. Levason, N. J. Hill and G. Reid, *J. Chem. Soc., Dalton Trans*., 2002, 4316–4317.

7. (a) A. J. Barton, N. J. Hill, W. Levason, B. Patel and G. Reid, *Chem. Commun*., 2001, 95–96; (b) A. J. Barton, N. J. Hill, W. Levason and G. Reid, *J. Chem. Soc., Dalton Trans.*, 2001, 1621–1627.
8. J. Zhang, Z. Peng, A. Soni, Y. Zhao, Y. Xiong, B. Peng, J. Wang, M. S. Dresselhaus and Q. Xiong, *Nano Lett.*, 2011, **11**, 2407–2414.
9. S. L. Benjamin, C. H. de Groot, A. L. Hector, R. Huang, E. Koukharenko, W. Levason and G. Reid, *J. Mater. Chem. C*, 2015, **3**, 423–430.
10. J. Wang, Z. Deng and Y. Li, *Mater. Res. Bull.*, 2002, **37**, 495–502.
11. A. Bera, K. Pal, D. V. S. Muthu, S. Sen, P. Guptasarma, U. V. Waghmare and A. K. Sood, *Phys. Rev. Lett.*, 2013, **110**, 1–5.
12. Z. G. Ivanova, E. Cernoskova, V. S. Vassilev and S. V. Boycheva, *Mater. Lett.*, 2003, **57**, 1025–1028.
13. G. C. Sosso, S. Caravati and M. Bernasconi, *J. Phys. Condens. Matter*, 2009, **21**, 095410 (6 pages).
14. N. Peranio, M. Winkler, Z. Aabdin, J. König, H. Böttner and O. Eibl, *Phys. Status Solidi A*, 2012, **209**, 289–293.
15. S. Zastrow, J. Gooth, T. Boehnert, S. Heiderich, W. Toellner, S. Heimann, S. Schulz and K. Nielsch, *Semicond. Sci. Technol.*, 2013, **28**, 035010 (6 pages).